Spontaneous 2D Accumulation of Charged Be Dopants in GaAs *p-n* Superlattices

S. Landrock,* K. Urban, and Ph. Ebert†

Institut für Festkörperforschung, Forschungszentrum Jülich GmbH, 52425 Jülich, Germany

(Received 16 November 2005; published 23 February 2006)

In a classical view, abrupt dopant profiles in semiconductors tend to be smoothed out by diffusion due to concentration gradients and repulsive screened Coulomb interactions between the charged dopants. We demonstrate, however, using cross-sectional scanning tunneling microscopy and secondary ion mass spectroscopy, that *charged* Be dopant atoms in GaAs *p-n* superlattices spontaneously accumulate and form two-dimensional dopant layers. These are stabilized by reduced repulsive screened Coulomb interactions between the charged dopants arising from the two-dimensional quantum mechanical confinement of charge carriers.

DOI: 10.1103/PhysRevLett.96.076101 PACS numbers: 68.55.Ln, 68.35.Fx, 73.61.Ey

As the size of semiconductor structures is rapidly shrinking, the nanoscale redistribution of dopant atoms becomes increasingly important for the properties of nanoelectronic devices [1]. In the conventional understanding, a concentration gradient as well as repulsive screened Coulomb interactions between the charged dopants lead to a redistribution of the dopants, widening and smoothing out steep dopant profiles. In this Letter we demonstrate, however, that beryllium (Be) dopant atoms in GaAs *p-n* superlattices accumulate in a self-organizing manner in two-dimensional layers, leading to steep dopant profiles at nanometer scales. We argue that these structures are stabilized by reduced screened Coulomb interactions between the charged dopants, due to the lower dimensionality. Furthermore, we illustrate that the dimensionality of the dopant structure strongly affects the diffusion kinetics.

As a model system we used molecular beam epitaxy (MBE) grown GaAs *p-n* superlattices doped with Be and silicon (Si), respectively. We investigated various layer thicknesses (10–100 nm), dopant concentrations (4×10^{18}–1.4×10^{19} cm^{-3}), and growth temperatures (720–830 K) using cross-sectional scanning tunneling microscopy (XSTM) and secondary ion mass spectroscopy (SIMS). Figure 1(a) shows an example of an XSTM image of several Be and Si-doped layers each with a nominal thickness of 50 nm. The *p* and *n*-doped regions are separated by darker lines, which arise from the depletion zones at the interfaces [2]. Although every layer should have the same thickness, the *p*-doped (brighter) layers are found to be enlarged by as much as 25% compared to the *n*-doped (darker) layers. Except for the first *p*-doped layer from the left, all other *p*-doped layers are surrounded by *n*-doped layers which have equal levels of dopant concentrations (1×10^{19} cm^{-3}). Therefore, the widening of the second to fourth *p*-doped layers is not due to a shift of the depletion zone arising from asymmetric doping levels [as, e.g., in [3]], but rather due to a real widening by diffusion.

The effect of diffusion is also visible in the corresponding SIMS spectrum for Be dopants shown in Fig. 1(b). While each Be-doped layer is enlarged in accordance with the above STM measurements, two well-developed maxima of the Be concentration occur near the interfaces towards the surrounding *n*-doped regions. The shape of this Be concentration profile differs significantly from the nominally grown structure shown as gray hatched bars. This indicates a strong redistribution of dopants by diffu-

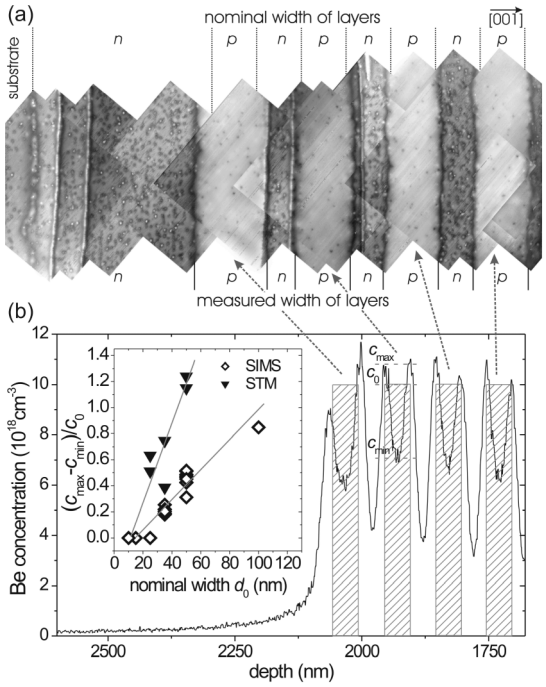

FIG. 1. (a) Mosaic of cross-sectional STM images of a GaAs *p-n* superlattice grown by MBE. On the far left the substrate and the *n*-doped buffer (Si: 4×10^{18} cm^{-3}) are visible followed by four *p*-doped layers (Be: 1×10^{19} cm^{-3}) separated by *n*-doped layers (Si: 1×10^{19} cm^{-3}). The nominally 50 nm wide *p*-doped layers (see dashed lines on the top) are significantly enlarged. (b) Corresponding SIMS spectrum for Be dopants. Each Be-doped layer exhibits a double maximum profile. The gray hatched bars indicate the nominally grown Be distribution. Inset: intensity of the double maximum structure plotted as normalized difference between the concentration of Be in the maxima and in the minimum, $(c_{max} - c_{min})/c_0$, vs the layer width measured by SIMS and STM.

sion. The open symbols in the inset of Fig. 1(b) illustrate furthermore that the degree of accumulation of dopant atoms in the two maxima [measured as the normalized difference between the concentration of Be in the maxima and in the minimum, $(c_{max} - c_{min})/c_0$] increases significantly with the nominal thickness of the p-doped layer. No redistribution of Si dopants was detected.

An accumulation of dopants was observed previously at p-n interfaces between Zn- and Si-doped regions by SIMS [4]. This effect was attributed to the formation of electrically neutral donor-acceptor pairs in the interface region due to Zn diffusion into the n-doped region [4,5]. However, since SIMS probes all dopants regardless of their electrical activity, no information about their charge state can be extracted. In particular, the degree of compensation and the spatial distribution of *charged* dopant atoms cannot be addressed.

The cross-sectional STM method allows us, however, to probe electronic properties with atomic resolution, such as the type of majority carriers [2] as well as the positions and charge states of individual dopants [6]. For example, the STM image in Fig. 1(a) shows that each p-type layer exhibits the same brightness in contrast in the center as well as near the interface regions. This indicates that the whole enlarged layer is now p type [2] including the edges near the interface regions, which were originally n doped. Thus, the diffusion of Be dopants leads not only to a compensation of the neighboring Si-doped regions by forming electrically inactive donor-acceptor complexes, but also to an overcompensation by introducing additional electrically active Be dopants.

This is further corroborated by high-resolution STM images [Fig. 2(a)], where every electrically active (negatively charged) Be dopant gives rise to a bright contrast due to the screened Coulomb potential. Figure 2(b) shows the projected positions of all charged Be dopant atoms in and a few layers below the surface. Thus Fig. 2 illustrates that negatively charged Be dopants are present outside the initially 50 nm thick grown p-doped layer, supporting the existence of overcompensation. Furthermore, an alignment of charged Be dopants near the interfaces is visible: the histogram of the charged Be dopant distribution (Fig. 3) shows a strong accumulation near the interfaces within the former n-doped regions. The resulting concentration of charged Be dopants near the interfaces exceeds the concentration in the center of the layer by nearly an order of magnitude. We observe that the degree of accumulation increases with increasing layer thickness [see solid symbols in the inset of Fig. 1(b)].

Note, in addition to the charged Be dopants (visible in STM images), one has to consider the presence of invisible uncharged dopants in concentrations of about 1×10^{19} cm^{-3}. The invisible dopants form uncharged Si-Be complexes compensating the Si dopants in the adjacent n-doped regions, as suggested by the difference of observed charged and initially grown-in dopants (Fig. 3). Thus, one has to distinguish between the accumulation of

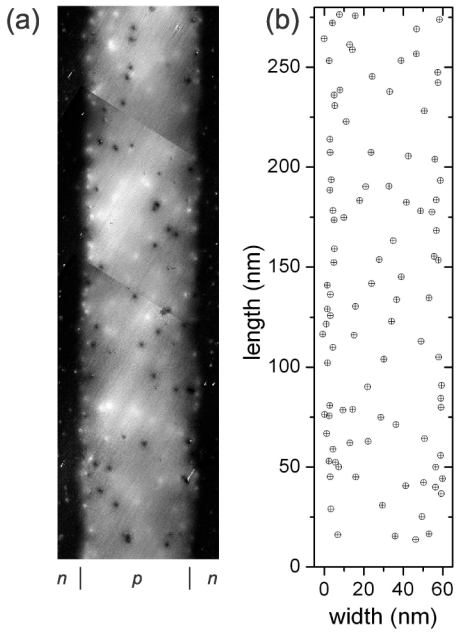

FIG. 2. (a) Contrast-enhanced cross-sectional STM image of a Be-doped layer in GaAs. The electrically active Be dopants are imaged as bright contrast features. The localized dark contrast features within the p-type layer are vacancies formed after cleavage of the sample. (b) Positions of the Be dopants in and a few layers below the surface extracted from (a).

charged Be dopants and that of Be atoms in electrically inactive Si-Be complexes. However, uncharged Si-Be complexes do not interact electrostatically with the charged dopant atoms.

At this stage, we focus on the stability of the Be dopant profiles by investigating the sample illustrated in Fig. 4(c). The corresponding SIMS profile in Fig. 4(b) shows that the two Be-doped layers (labeled 2 and 4) embedded in undoped *intrinsic* GaAs exhibit a normal Gaussian-like profile. The width of these layers increases with time t at the growth temperature of about 770 K [compare broadening of layers 2 and 4 in Fig. 4(a)]. In contrast, the two Be-doped layers surrounded by Si-doped GaAs (labeled 1 and 3) exhibit a double maximum profile. These layers essentially stop becoming broader with time [Fig. 4(a)]. In a first order approximation the layer broadening of a Be-doped layer Δd is proportional to $\sqrt{Dt}$ with D being the diffusion coefficient [7]. Thus the slopes in Fig. 4(a) indicate a smaller diffusion coefficient for Be layers embedded in Si-doped GaAs in comparison to the case of normal diffusion without Si counterdoping. This corroborates the existence of a strongly retarded diffusion once a double maximum profile is present. As a result, the remarkable accumulation of charged Be dopants near the p-n junctions is unaltered over long periods of time even at high growth temperatures.

However, the double maximum profile itself forms rather quickly: even the layers exposed briefly (<30 min) to the growth temperature exhibit fully developed double

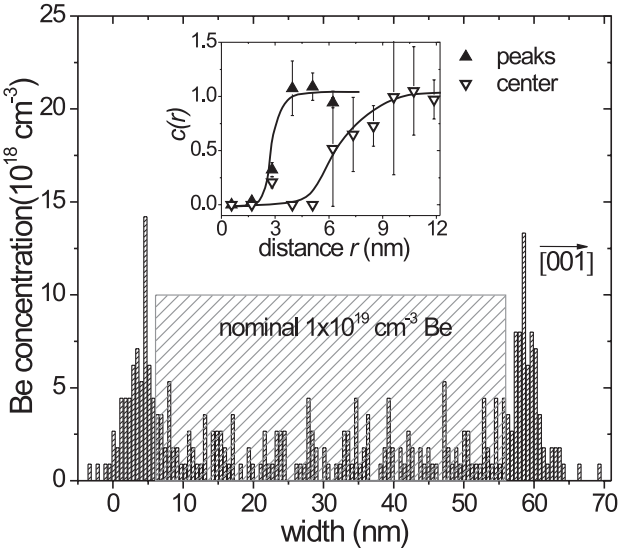

FIG. 3. Distribution of charged Be dopants along the growth direction. Strong accumulations occur near the interface. The gray hatched area indicates the nominally grown Be profile. Note that the total number of charged Be atoms is much lower than that nominally grown in, because most Be dopants compensate Si dopants in the adjacent initially n-doped layers by forming uncharged Si-Be complexes, which are invisible in STM images. For this plot the positions of 323 Be dopants were evaluated. Inset: pair-correlation function $c(r)$ for charged dopants in the center of the layer and in the accumulation peaks. The lines are a guide to the eye.

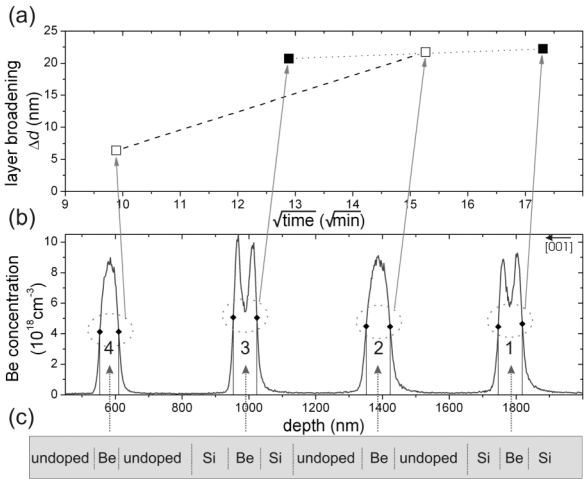

FIG. 4. (a) Broadening as a function of $\sqrt{\text{time}}$ of nominally 50 nm thick Be-doped layers embedded in undoped GaAs (labeled 2 and 4, open symbols) and in Si-doped GaAs (labeled 1 and 3, solid symbols). (b) Be profile measured by SIMS, showing the corresponding Gaussian-like and double maximum profiles, respectively. (c) Schematic of the sample. The data suggest a retarded diffusion for layers 1 and 3. Furthermore, Si counterdoping is essential for the formation of double maximum profiles.

maximum profiles similar to those of the layers exposed extensively ($\approx$7 h). This suggests an initially considerably enhanced diffusion changing into a retarded diffusion once the double maximum profiles are formed. Note, Fig. 4 illustrates also that the Si counterdoping is essential for the formation of a double maximum profile.

The experimental results presented above raise a puzzling issue. A double maximum profile of *charged* dopant atoms as found in Fig. 3 should not be stable: equally charged dopant atoms should repel each other and there should be a diffusion along the concentration gradient. Both effects should smooth out the steep doping profiles and thus remove the accumulation of charged dopants near the interfaces.

In order to address this issue, we first discuss the atomistic processes involved in diffusion. During MBE growth the Fermi energy E_F at the n-doped growth surface is pinned at midgap position [8]. A newly grown n-doped GaAs layer will thus initially exhibit intrinsic characteristics, which change, while growth proceeds and the distance from the growth surface increases, towards n-type properties. The closer the conduction band edge gets to the Fermi energy, the more Ga vacancies (V_{Ga}) are formed according to the Fermi-level effect [9]. This process $\mathrm{Ga_{Ga}} \rightarrow V_{\mathrm{Ga}}^{3-} + \mathrm{Ga}_i^{+} + 2h^{+}$ leads to the formation of positively charged Ga interstitials (Ga_i^{+}). The built-in electric field of the p-n junction drives the Ga_i^{+} preferentially towards the p-doped layers [8,10]. Because of the Coulomb attraction between the negatively charged $\mathrm{Be}_{\mathrm{Ga}}^{-}$ dopants and the positively charged Ga_i^{+}, the Ga_i^{+} preferentially kick out the Be dopants by $\mathrm{Be_{Ga}} + \mathrm{Ga}_i \rightarrow \mathrm{Be}_i + \mathrm{Ga_{Ga}}$ producing Be interstitials Be_i. These are highly mobile [11], which is consistent with the observed enhanced diffusion leading to the rapid appearance of the double maximum Be profiles. Statistically the Be_i diffuse into the n-doped layer, where they form uncharged Si-Be complexes either by filling a Ga vacancy or by kicking out a Ga atom. The latter further fuels the enhanced diffusion by forming new Ga_i^{+}. Note that the presence of the neighboring Si-doped regions is thus the origin of the enhanced diffusion. This is consistent with the data in Fig. 4.

In addition to the formation of uncharged Si-Be complexes, electrically active Be dopants accumulate at the edges of the widened Be-doped regions (Fig. 3), overcompensating the initially n-doped regions. The massive accumulations of *charged* Be dopants push the depletion zones into the remaining n-doped layers, such that the Fermi level moves towards midgap. Due to the Fermi-level effect the V_{Ga} concentration then decreases in the n-doped layer by eliminating the remaining Ga_i [9] and the whole enhanced diffusion process comes to a halt.

We recall that directly after the enhanced diffusion has come to a halt, a strongly retarded diffusion regime stabilizes the remarkable accumulation of charged Be dopants. In order to address the stability, we discuss the formation energy E_{form} of a $\mathrm{Be}_{\mathrm{Ga}}^{-}$ in GaAs, which is given by [12] $E^{\mathrm{form}} = E^{\mathrm{tot}} - \sum_i N_i \mu_i + qE_F + qV^{\mathrm{Int}}$ with q being the charge of the dopant and N_i and μ_i being the particle

numbers and chemical potentials, respectively, of all components i involved. Only the last two terms are relevant for stabilizing the accumulation of charged Be dopants. As mentioned above, this accumulation pushes the depletion zone primarily into the n-doped region. Thus within the Be-doped layer the effect of a changing E_F is negligible. The remaining term arises from the repulsive electrostatic interaction potential V^{Int} between the charged dopants, governed by the screening length R_S [13,14]. For three-dimensional dopant interactions we found, however, that at growth temperature no energy can be gained (due to reduced interactions) if the dopant distribution undergoes a phase separation into high- and low-doped layers. This is due to the fact that the average separation between the dopant atoms decreases faster with increasing dopant concentrations ($>10^{18}$ cm^{-3}) than the three-dimensional bulk screening length.

However, the screened Coulomb interactions can be lowered drastically if a two-dimensional screening system exists. A GaAs layer exhibits a two-dimensional character for charge carriers if its thickness is smaller than the thermal de Broglie wavelength $\lambda = h/\sqrt{2mk_BT}$ [7]. For holes in GaAs the de Broglie wavelength at the growth temperatures of $T \approx 800$ K is in the range of 6 to 7 nm, matching the thickness of the charged Be accumulation layers (Fig. 3). This indicates that the dopant atoms have condensed into electronic two-dimensional layers, confining the holes. The reduction of the dimension by quantum confinement leads to a two-dimensional density of states. As a consequence the screening length is reduced to about 0.6 nm [2D screening length $\approx(2\pi\epsilon_0\epsilon_r\hbar^2)/(e^2m)$ [15]] instead of 2.2 to 4.9 nm for three-dimensional screening at 800 K for carrier concentrations of $(0.2\text{–}1) \times 10^{19}$ cm^{-3} [13]. The decrease of the screening length is also corroborated by the measured pair-correlation functions (Fig. 3 inset), which show a reduced interaction range within the charged Be accumulation layers. Thus the extension of the repulsive interaction potential is shortened significantly by the condensation of dopant atoms into two-dimensional layers, lowering the formation energy of a dopant and thus allowing more dopants to be incorporated before repulsive interactions become relevant.

The two-dimensional confinement of charge carriers has further consequences: if a dopant migrates away from its position within the accumulation layer, its energy increases due to growing interactions. Thus the dopant experiences forces driving it back towards the two-dimensional dopant layer. This slows down a further widening of the Be profile and leads to the observed retarded diffusion.

The degree of condensation into two-dimensional doping layers increases with increasing layer thickness (see inset in Fig. 1). The extrapolation of the measured data indicates that the driving force for condensation vanishes for layers with thicknesses in the range of 12 ± 5 nm, which is roughly twice the de Broglie wavelength. In such a case there is no space for two separate two-dimensional dopant accumulation layers. This is corroborated by the observation that 15 nm wide layers do not exhibit a redistribution of dopant atoms.

Our results raise the question of whether 2D accumulations of charged dopants can occur in other semiconductor systems, too. III-V semiconductor systems with p-type dopants substituting cations and diffusing via a kick-out mechanism should exhibit similar charged dopant accumulations near p-n interfaces. This is corroborated, for example, by SIMS profiles measured for Zn in InP p-n junctions [4], which are similar to those of Be in GaAs, suggesting a similar diffusion mechanism and thus the possibility of 2D accumulations of charged Zn dopants.

In conclusion, we have demonstrated that charged Be dopant atoms in GaAs p-n superlattices accumulate spontaneously near the p-n interfaces and form two-dimensional doping layers. These are stabilized by the two-dimensional quantum mechanical confinement of charge carriers, which leads to a reduced screening length and thus to reduced repulsive screened Coulomb interactions between the charged dopants. The formation energy of a charged Be dopant can therefore be lowered by reducing the dimensionality of the dopant structure. This also leads to a strongly retarded diffusion after an initially enhanced diffusion.

The authors thank C. Krause and A. Förster for growing the samples, U. Breuer for the SIMS measurements, K. H. Graf for technical support, and the Deutsche Forschungsgemeinschaft as well as the German-Israeli Foundation for financial support.

*Electronic address: S.Landrock@fz-juelich.de
†Electronic address: P.Ebert@fz-juelich.de

[1] S. Roy and A. Asenov, Science **309**, 388 (2005).
[2] N. D. Jäger, M. Marso, M. Salmeron, E. R. Weber, K. Urban, and Ph. Ebert, Phys. Rev. B **67**, 165307 (2003).
[3] R. M. Feenstra, E. T. Yu, J. Woodall, P. Kirchner, C. Lin, and G. Pettit, Appl. Phys. Lett. **61**, 795 (1992).
[4] C. Blauuw, F. R. Sheperd, and D. Eger, J. Appl. Phys. **66**, 605 (1989).
[5] S. J. Taylor, B. Beaumont, and J. C. Guillaume, Semicond. Sci. Technol. **8**, 643 (1993).
[6] Ph. Ebert, Surf. Sci. Rep. **33**, 121 (1999).
[7] E. F. Schubert, *Delta-Doping of Semiconductors* (Cambridge University Press, Cambridge, England, 1996).
[8] D. G. Deppe, Appl. Phys. Lett. **56**, 370 (1990).
[9] T. Y. Tan and U. Gösele, Appl. Phys. Lett. **52**, 1240 (1988).
[10] C. Y. Chen, R. M. Cohen, D. S. Simons, and P. H. Chi, Appl. Phys. Lett. **67**, 10 (1995).
[11] S. Yu, T. Y. Tan, and U. Gösele, J. Appl. Phys. **69**, 3547 (1991).
[12] J. E. Northrup and S. B. Zhang, Phys. Rev. B **47**, 6791 (1993).
[13] R. B. Dingle, Philos. Mag. **46**, 831 (1955).
[14] Ph. Ebert, T. J. Zhang, F. Kluge, M. Simon, Z. Y. Zhang, and K. Urban, Phys. Rev. Lett. **83**, 757 (1999).
[15] F. Stern and W. E. Howard, Phys. Rev. **163**, 816 (1967).